

Journal of Materials Chemistry B

Accepted Manuscript



This is an *Accepted Manuscript*, which has been through the Royal Society of Chemistry peer review process and has been accepted for publication.

Accepted Manuscripts are published online shortly after acceptance, before technical editing, formatting and proof reading. Using this free service, authors can make their results available to the community, in citable form, before we publish the edited article. We will replace this *Accepted Manuscript* with the edited and formatted *Advance Article* as soon as it is available.

You can find more information about *Accepted Manuscripts* in the [Information for Authors](#).

Please note that technical editing may introduce minor changes to the text and/or graphics, which may alter content. The journal's standard [Terms & Conditions](#) and the [Ethical guidelines](#) still apply. In no event shall the Royal Society of Chemistry be held responsible for any errors or omissions in this *Accepted Manuscript* or any consequences arising from the use of any information it contains.

ARTICLE

Mesoporous silica nanoparticles grafted with light-responsive protein shell for highly cytotoxic antitumoral therapy.

Cite this: DOI: 10.1039/x0xx00000x

Received 00th January 2012,
Accepted 00th January 2012

DOI: 10.1039/x0xx00000x

www.rsc.org/

Marina Martínez-Carmona^a, Alejandro Baeza^{a,*}, Miguel A. Rodríguez-Milla^b,
Javier García-Castro^b and María Vallet-Regí^{a,*}

A novel phototriggered drug delivery nanocarrier which exhibits very high tumor cytotoxicity against human tumoral cells is presented. This device is based on mesoporous silica nanoparticles decorated with a biocompatible protein shell cleavable by light irradiation. The proteins which compose the protein shell (avidin, streptavidin and biotinylated transferrin) acts as targeting and capping agents at the same time, avoiding the use of redundant systems. The light responsive behavior is provided by a biotinylated photocleavable cross-linker covalently grafted on the mesoporous surface which suffers photocleavage by UV radiation (366 nm). Human tumoral cells incubated in the presence of a very low particle concentration enter into apoptotic stage after a short irradiation time. Thus, the system here described could be applied for the treatment of exposed tumors that affect to skin, esophagous, stomach, among others, which can be easily accessible for light irradiation.

Introduction

In the recent years, nanoparticles with a size range of 1-500 nm have offered a novel alternative to traditional therapy in oncology.^[1] Most of the conventional chemotherapeutic agents have poor pharmacokinetic profiles and are distributed non-specifically in the body, leading to systemic toxicity associated with serious side effects.^[2] Therefore, great efforts have been carried out for the development of nanocarriers able to transport and deliver multiple therapeutic agents, specifically to defined target cells without affecting the healthy ones.^[3] Tumor blood vessels are different to normal ones; due to its rapid and chaotic growth, they have abnormal architectures which present large fenestrations with diameters up to few hundred nanometers, being highly permeable. This anatomical defectiveness promotes the extravasation of nanoparticles through these pores causing their tumoral tissue accumulation.^[4] Moreover, the slow venous return and the poor lymphatic clearance characteristic of neoplastic tissues mean that particles remain trapped during longer times. Both behaviors, high permeability and poor lymphatic drainage, constitute the gold standard of the use of nanoparticles for antitumoral therapy because they lead to a passive accumulation of the nanocarriers within the tumoral tissue by a phenomenon called EPR effect (*enhanced permeability and*

retention).^[5] To improve the selectivity of the nanoparticles against the diseased cells, the external surface of the nanoparticles can be decorated with different molecules able to be selectively recognized by the tumoral cells as antibodies, proteins, oligonucleotides or small molecules, among others.^[6] Additionally, if drug release takes place once internalized within the tumoral cell, the cytotoxic effect of the released drug could be stronger as a consequence of the reduced volume of the cell. This behavior may be achieved using stimuli-responsive nanodevices able to release their therapeutic payloads only in the presence of certain stimulus.^[7] Mesoporous silica nanoparticles (MSN) have attracted much attention because of their unique properties.^[8-10] Additionally, this material can be functionalized with stimuli-responsive gatekeepers placed outside the pore openings in order to control or trigger the drug release by the presence of a specific stimulus.^[11] Thus, many inorganic or organic moieties such as nanocrystals,^[12] DNA,^[13] proteins,^[14] polymers^[15] or small molecules,^[16,17] among others have been employed as responsive gates to different stimuli. Among these stimuli, light is a powerful tool because it presents low toxicity and its application can be spatially and temporally controlled by finely selecting the area and the exposure time.^[18,19] Moreover, light can be locally applied to internal tumor areas using optic probes. Fujiwara *et al.*^[20] described by the first time the use of light sensitive MSN

placing coumarin molecules on the pore outlets. These molecules suffer dimerization which blocks the pore in a reversible way in response to light irradiation. Later, other moieties have been grafted on MSN surface using light-cleavable bonds.^[21-23] However, it has been observed that certain capping agents (metal nanoparticles, dendrimers, cationic polymers, etc.) themselves may cause cytotoxic damage to host.^[24-26] Proteins are compatible with biological systems, biodegradable, nontoxic and non-immunogenic as well as very stable, and really specific.^[27] Herein, we propose a novel photosensitive drug delivery nanocarrier based on mesoporous silica particles covered with a photosensitive protein shell cleavable by light irradiation. Moreover, in order to avoid the use of redundant systems, the external protein layer acts as targeting and capping agents at the same time (**Figure 1**).

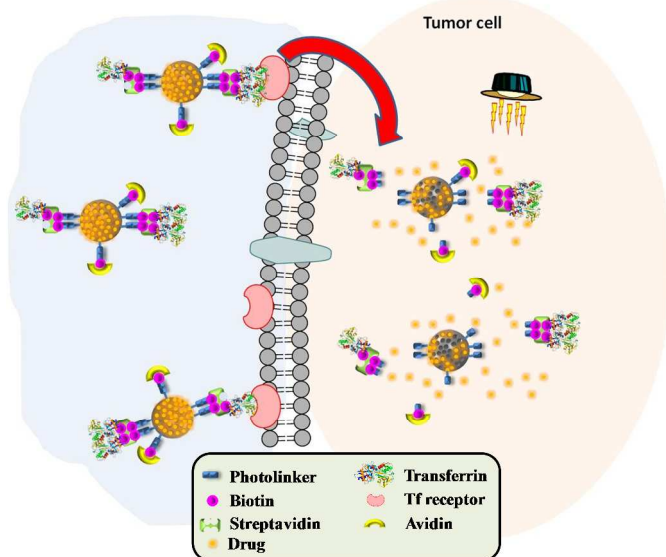


Figure 1. Schematic illustration of the action mechanism of the light-responsive device

MSN surface was decorated with a light-sensitive cross-linker whose biocompatibility has been also proved (both the residues before and after photocleavage)^[28] which carried biotin moieties. Thus, the proteins which compose the protein shell (avidin, streptavidin and biotinylated transferrin) were attached on the MSN surface by avidin/streptavidin-biotin interactions. The supramolecular interaction between avidin or streptavidin and biotin is one of the strongest non-covalent biological interaction known ($K_d = 4 \times 10^{-14}$ M), being the bond formed very rapidly and keeping stable in wide ranges of pH and temperature.^[29-31] The targeting capacity of the device was provided by the attachment of transferrin (Tf) molecules on the MSN surface using previously biotinylated transferrin. The transferrin receptor functions in cellular iron uptake through its interaction with Tf. This receptor is an attractive molecule for the targeted therapy of cancer since it is upregulated on the surface of many cancer types.^[32-34] It has been widely reported that the presence of transferrin in the surface displays enhancement in particle uptake of different nanosystems into human cells.^[35-38] It is important to highlight the simplicity of our device where the protein shell perform a dual function as

gatekeeper and targeting agent at the same time. The nanodevice here presented corresponds to a proof of concept of the potential antitumoral clinical applications of these types of systems. Finally, the presence of photocleavable biotins on the surface introduces high versatility due to it is also possible to attach other targeting agents and therapeutic macromolecules using biotin-streptavidin bridges.

Results and Discussion

Synthesis of biotinylated MSN

For this purpose, MSN were prepared according to a modified Stöber method producing round shaped particles with diameters around 120 nm.^[39] For the synthesis of the photosensitive cross-linker, biotin was coupled with the commercially available photolinker previously deprotected (PhoL1) using carbodiimide chemistry. Once isolated the biotin-photolinker compound (PhoL2) aminopropyltriethoxysilane (APTES) was reacted with the activated acid group using a similar strategy, producing the final compound (PhoL3). The reaction product was confirmed by ¹H-NMR (**Figure 2**).

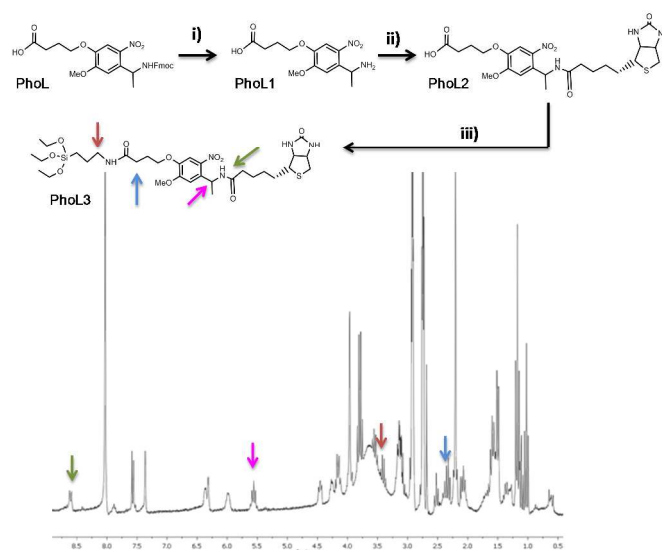
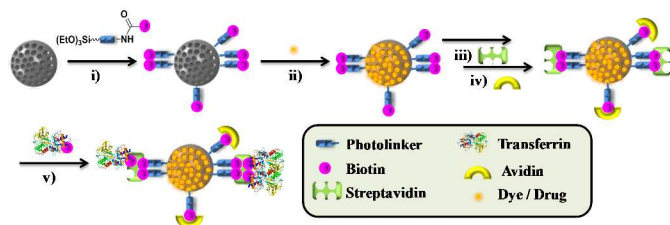


Figure 2. Scheme of synthesis and H-NMR spectrum of PhoL3. i) piperidine / DMF (20%), ii) (+)-Biotin N-hydroxysuccinimide ester, iii) APTES

The appearance of a new signal at 8.5 ppm due to the amide formation between the amino group of the biotin and the carboxylic acid of the PhoL was observed (green arrow). It is also possible to observe that the nearest methylene protons (CH_2 , red arrow and CH , purple arrow) of the new amide bonds shift to lower fields. Additionally, the methylene group close to carbonyl (blue arrow) suffers shift to higher fields as a consequence of the new amide bond formation (For complete proton assignment see **(Figure S1-3)**). The formation of PhoL3 was also confirmed by FTIR and mass spectrometry (**Figure S4 and S5**). MSN surface was decorated with PhoL3 by refluxing in toluene during 12 hours in darkness conditions producing the functionalized particles (MSN-B).

[Ru(bipy)₃]Cl₂ loading and capping

To test the feasibility of the light-responsive behavior 50 mg of MSN-B were loaded with [Ru(bipy)₃]Cl₂ as fluorophore for 36 hours. After that, particles were capped with streptavidin, avidin and biotinylated transferrin which were added sequentially at 1 hour intervals and finally allowed to react overnight in a refrigerator (**Scheme 1**).



Scheme 1. Synthesis of the nanocarrier MSN-Tf. i) PhoL3, ii) [Ru(bipy)₃]Cl₂ or Dox, iii) streptavidin, iv) avidin, biotinylated transferrin.

Avidin was employed in order to bind to the excess of the biotin non complexed with streptavidin guaranteeing the pore capping. The excess [Ru(bipy)₃]Cl₂ was removed by filtration, centrifugation and washing with water. The product, MSN-Tf-Ru, was dried in a N₂ flow.

Light-responsive release

In order to monitor the light-responsive behavior, two batches of MSN-Tf-Ru particles were suspended in water and one of them was exposed to 366 nm irradiation for 15 min and stirred during 1h. The other batch was treated under similar conditions but without light irradiation. The amount of fluorophore released was determined by fluorescence measurements of the solutions, ($\lambda_{\text{ex}} = 451 \text{ nm}$, $\lambda_{\text{em}} = 619 \text{ nm}$). The released dye for both the irradiated and non-irradiated samples is shown in **Figure 3a** showing a remarkable fluorescence increase in the case of the illuminated sample. This experiment was carried out twice displaying similar results. To ensure that the drug release is triggered by the light-induced protein shell removal, the previous experiment was repeated but without dye loading of MSN-B and using fluorescent labeled Tf which allows an easy monitorization of the uncapping process by fluorescence spectroscopy. Similar to the previous case, the observed fluorescence with irradiated sample was markedly higher than the sample remained in darkness (**Figure 3b**).

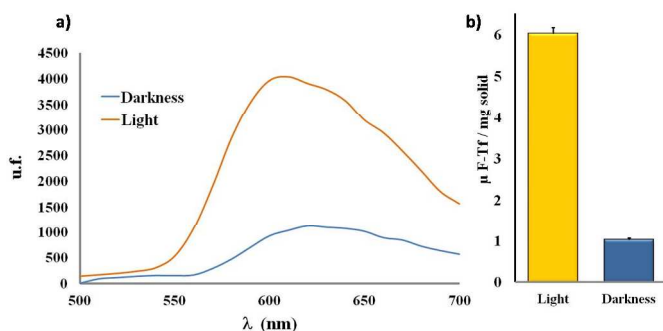


Figure 3. a) [Ru(bipy)₃]Cl₂ release of MSN-Tf-Ru and b) fluorescent labeled Tf release from MSN-Tf in the absence of light and upon UV light irradiation.

MSN-Tf characterization

In order to perform a better characterization of the complete material, MSN-Tf was synthesized without loading dyes. MSN, MSN-B and MSN-Tf were characterized by different techniques and the results compared after each reaction step. By FTIR spectroscopy we were able to follow the nanoparticle coating process. The change from a clean spectrum in the 1500-2000 cm⁻¹ range of MSN to the presence of two signals at 1637 and 1519 cm⁻¹ characteristic of PhoL3 in MSN-B was observed (**Figure S6**). Finally in the FTIR spectrum of MSN-Tf, a broadening of the bands mentioned above as well as a clear increase in intensity corresponding to the presence of a greater number of amide bonds is appreciated. The functionalization degree of the particles was calculated by difference between thermogravimetric analysis (TGA) measures finding 16% of PhoL3 in MSN-B and 6% of protein shell in the final system MSN-Tf. As it would be expected, the pore volume of the mesoporous silica material suffers a significant decrease with increasing surface decoration. Thus, the specific surface area changes from 952 in the case of naked material (MSN) to 121 m²/g, in the case of the complete system MSN-Tf (**Figure S7**). The porosity network also experiment a significant order loss as a consequence of the protein shell formation (**Figure S8**). The size of the different nanoparticles was determined by dynamic light scattering (DLS) showing that the sized distribution shifted to higher values (122 to 190 nm) with increasing functionalization (**Figure 4a**). As can be observed in **Figure S9** by increasing the functionalization the sample becomes less homogeneous thereby increasing lightly its polydispersity index (PDI) (**Table S2**).

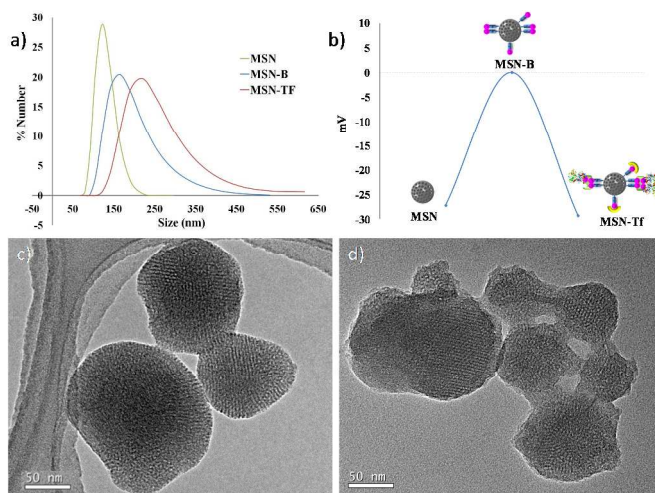


Figure 4. a) DLS and b) Z potential measurements of MSN materials. c-d) TEM images of MSN and MSN-Tf respectively

Zeta potential measurements in water of these particles show drastic change on the superficial charge with values of -27.2, +0.02 and -29.3 mV for MSN, MSN-B and MSN-Tf, respectively (**Figure 4b**). This is consistent with the expected results because biotinylation introduce hydrophobicity on the surface and therefore, the surface charge in water approaches to

zero. After the transferrin and avidin grafting step, the surface charge of the particle becomes negative again due to the negatively charged nature of the introduced proteins at neutral pH as a consequence of their isoelectric points (PI) which are 5.5 and 6.7, respectively. Finally, it was possible to observe the protein shell by transmission electron microscopy (TEM). **Figure 4c-d** shows the transition from a smooth (MSN) to rough (MSN-Tf) surface of the particles.

Dox loading and capping

Once the system was fully characterized and proved to work properly, particles were loaded with Doxorubicin (Dox) in order to test their antitumoral properties using cell cultures. Doxorubicin was loaded into the pores of the material by soaking dried MSN-B in a solution of Dox (3 mg/ml) for 48h. After that, the system was sealed by the addition of proteins following the procedure previously described. The excess Dox was removed by filtration, centrifugation and washing with water. The product, MSN-Tf-Dox, was dried in a N₂ flow at room temperature. The amount of Dox loaded in the sample was determined from the difference between the fluorescence measurements of the initial and the recovered filtrate solutions. The results indicate that MSN-Tf-Dox present a loading capacity around 7% w/w.

In Vitro Cytotoxicity and Cellular Uptake Evaluation

As it was mentioned, transferrin receptor is known to be overexpressed in many cancer cell lines. The amount of transferrin receptors was determined in four different tumoral cell lines of Ewin tumor (A673) fibrosarcoma (HT1080) osteosarcoma (SAOS2) and neuroblastoma (NB1681) in order to select one of them which show the higher affinity by transferrin molecule. HT1080 tumoral cell line was chosen in the first trials due to transferrin receptors are expressed in the higher amount (**Figure S10**).

In order to test the targeting capacity of the transferrin placed on the external surface of the carriers, HT1080 cells were incubated in the presence of particles functionalized with transferrin (MSN-Tf) and naked ones (MSN). Both type of particles were labeled with fluorescein through conjugation with fluorescein isothiocyanate (FITC) as has been previously reported.^[40] Thus, HT1080 cells were exposed to a certain amount of fluorescent nanoparticles during 24 hours. The amount of cells which engulf particles was determined by flow cytometry. Particles functionalized with the protein shell show a five-fold increase in cell uptake in comparison with the non-functionalized system (**Figure 5a**). Confocal images demonstrate that nanoparticles were efficiently internalized inside of HT1080 tumoral cells (**Figure 5b**). Particle internalization was not observed when the cells were treated with particles without the protein shell on the surface.

The *in vitro* cytotoxicity study of the system was determined by the exposition of this cellular line to increased amounts of nanomaterials functionalized with transferrin and loaded with doxorubicin (MSN-Tf-Dox) with and without light irradiation

in order to establish the minimal concentration required to induce significant cellular apoptosis.

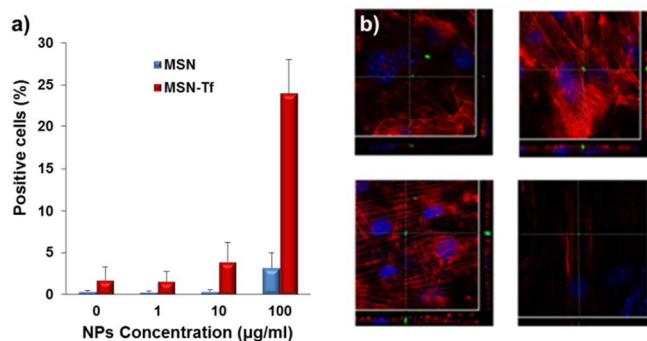


Figure 5. a) Cellular uptake of MSN and MSN-Tf labeled with fluorescein, b) Confocal microscopy images showing nanoparticles (green) inside of HT1080 cells (actin in red, nucleus in blue) The bottom and side panels show the x-z and y-z cross-sectional images, respectively.

Cells were incubated during 24 hours in order to allow the particle uptake. After this time, the cells were washed with PBS for removing the non-internalized particles and the premature released drug. Then, one batch of cells was exposed to 15 min of light irradiation maintaining the other batch in darkness conditions.

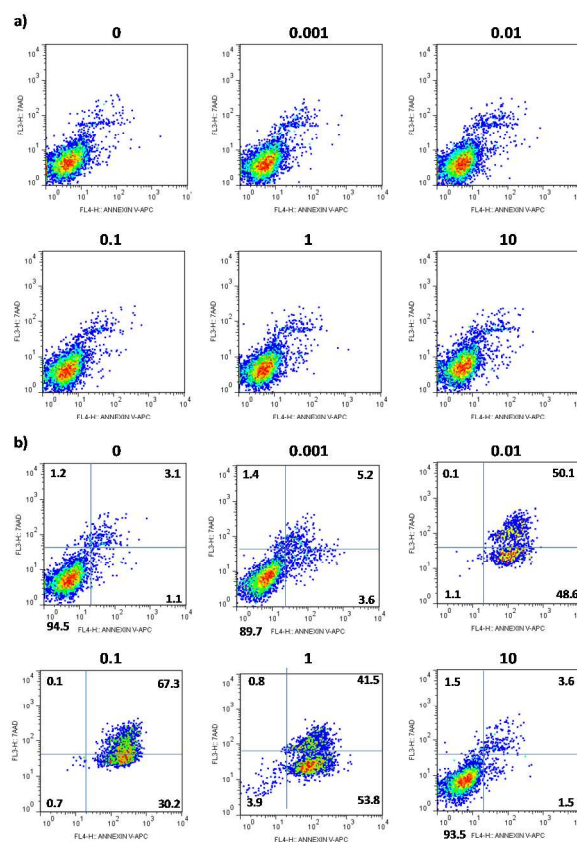


Figure 6. a) Flow cytometry of HT1080 cells treated with MSN-Tf-Dox without UV irradiation, stained with Annexin-V and 7-AAD. Upper number: Doses of Doxorubicin in µg/mL. b) Flow cytometry of HT1080 cells treated with MSN-Tf-Dox irradiated with UV light, stained with Annexin-V and 7-AAD. Upper number: Doses of Doxorubicin in µg/mL.

After two days of incubation time, the cytotoxicity was evaluated by flow cytometry using Annexin V/7-AAD protocol for apoptotic cell determination. As is shown in **Figure 6b**, a clear apoptosis is seen in the 100% of cells with nanoparticle doses so lower as 0.01 $\mu\text{g}/\text{mL}$ and UV irradiation, whereas the samples which were maintained in darkness conditions present a same survival ratio than the controls (**Figure 6a**). The reported IC₅₀ value of free doxorubicin in HT1080 cells is 0.006 $\mu\text{g}\cdot\text{mL}^{-1}$.^[41] This fact means almost ten-fold enhance of the therapeutic efficacy of the drug due to 0.01 $\mu\text{g}\cdot\text{mL}^{-1}$ of particles release at the most 0.0007 $\mu\text{g}\cdot\text{mL}^{-1}$ according with the maximum loading mentioned above. It is important to note that cells were not affected by the simply exposition of UV light without particles. Similar results were obtained with nanoparticles loaded with other cytotoxic drug, oxaliplatin (**Figure S11** and **S12**). Finally, the other three tumoral cell lines were exposed to the presence of these doxorubicin loaded nanoparticles in order to test if this system is able to destroy other tumoral cell lines which express lower amount of transferrin receptors on their surface (**Figure S10**). In all the cases, the cells entered in apoptotic state when equivalent amounts of drug loaded nanoparticles were employed under light irradiation conditions. These data suggest that the nanoparticles are able to be efficiently internalized in the cells independently of the amount of transferrin receptors. The ubiquitous nature of transferrin receptors which are present also in many healthy cells could be a drawback of the use of transferrin as targeting agent.^[42,43] In our device, transferrin plays a dual role being a capping agent that prevents the premature departure of the loaded drug and a cell uptake enhancer. Drug departure is taking place only after light irradiation which could avoid the apparition of side effects in healthy cells as a consequence of the fact that light can be easily focused only in the diseased tissue. These data clearly indicate that nanoparticles are able to induce apoptosis at really low dosages which could be of great interest for oncological applications.

Experimental Section

Synthesis of mesoporous silica nanoparticles (MSN)

MSN were synthesized as following: to a 1 L round-bottom flask, 1 g of CTAB as a structure-directing agent, 480 mL of H₂O (Milli-Q), 3.5 mL of NaOH (2 M) were added. The mixture was heated to 80°C and stirred at 600 rpm. When the reaction mixture was stabilized at 80°C, 5 mL of TEOS were added dropwise at 0.33 mL/min rate. The white suspension obtained was stirred during further 2h at 80°C. The reaction mixture was filtered and washed 3 times with 100 mL of H₂O, and then ones with 50 mL of EtOH. Finally, the surfactant was removed by ionic exchange using a solution of ammonium nitrate (10 mg/mL) in 400 mL of ethanol (95%) at 65°C overnight under magnetic stirring.

Synthesis of fluorescent MSN

FITC (1mg) and APTES (2,2 μL) were dissolved in the minimum volume of EtOH and the mixture was stirring at room temperature for 2 hours under N₂ atmosphere. The resulting solution was called Solution 1. Fluorescent MSN were synthesized following the same procedure used for MSN but instead of adding 5 mL of TEOS, a mixture of 5 mL of TEOS and Solution 1 was used.

Synthesis of PhoL1

600 mg of Fmoc-photolinker were placed in a 25 mL round bottom flask and dissolved in 12 mL of piperidine/DMF (20%) solution. The flask was placed in an ultrasound bath for 1h in the absence of light to remove the protecting group. Solvent was evaporated in a rotavap using a cannula and the product was washed with ether, filtrated and dried in a vacuum oven at 40°C overnight.

Synthesis of PhoL2

200 mg of photolinker were placed in a 100 mL round bottom flask and dissolved in 38 mL of dry DMF. 250 mg of NHS-B were added and the solution was stirred in darkness at room temperature for 2 h. Solvent was evaporated in the rotavap using a cannula, the product was washed with ether, filtrated and dried in a vacuum oven at 40°C overnight.

Synthesis of PhoL3

350 mg of PhoL2 were placed in a 100 mL round bottom flask and dissolved in 38 mL of dry DMF. To this solution, 106 mg of DCC and 99 mg of NHS were added and the mixer was stirred in darkness at room temperature for 2 h. After that 223 μL of APTES were added and the reaction was allow to stir for 3h at room temperature. The precipitated dicyclohexylurea was removed by filtration and solvent was evaporated in the rotavap using a cannula, the product was washed with ether, filtrated and dried in a vacuum oven at 40°C overnight.

Attachment of PhoL3 on the MSN

350 mg of MSN were placed in a three-neck round bottom flask and dried at 80°C under vacuum for 24 h. Then, 125 mL of dry toluene were added and the flask was placed in an ultrasonic bath for better suspension of particles. After that a solution of 210 mg of PhoL3 in 28 mL of dry DMF were added, keeping the reaction in darkness, under nitrogen atmosphere at 80°C for 24h. After that time, the sample was filtered and washed two times with water and once with MeOH. Finally, the product was dried under vacuum at 40°C.

Synthesis of biotinylated Tf

To a solution of 5 mg transferrin in 1mL of PBS 1mg of (+)-Biotin *N*-hydroxysuccinimide ester (NHS-B) dissolved in 10 μL of DMSO was added. The solution was stirred for 2 h. The protein was purified by centrifugal separation with 30KDa cut-off filters (AMICON®

Ultra-2 30K) and washed three times with fresh phosphate buffer saline (PBS). The protein was concentrated to final volume of 200 μ L.

Synthesis of fluorescence Tf

1 mg of biotinylated Tf was dissolved in 1 ml of PBS buffer. Then 10 μ L of a solution of 1 mg of FITC dissolved in 100 μ L of DMSO was added. The reaction mixture was stirred at 250 r.p.m. for 2 h at room temperature. The protein was purified by centrifugal separation with 50KDa cut-off filters (AMICON® Ultra-2 50K) and washed three times with PBS buffer. The protein was concentrated to final volume of 250 μ L.

[Ru(bipy)₃]Cl₂ / Dox loading and capping (MSN-Tf)

50 mg of MSN were placed in a topaz vial and dried at 80°C under vacuum overnight. Then, 7 mL of [Ru(bipy)₃]Cl₂ or Dox aqueous solution (10 or 3 mg/mL respectively) were added and the suspension was stirred at room temperature for 48 h. After that, particles were capped with 2.5 mg of streptavidin, 25 mg of avidin and 200 μ L of biotinylated transferrin and that were added sequentially at 1 hour intervals and finally allowed to react overnight in a refrigerator. Then, samples were filtered and washed two times with water (2x2 mL) in order to remove the [Ru(bipy)₃]Cl₂ or Dox absorbed on the external surface. Finally, the products were dried under vacuum at 25°C. A similar loading procedure was employed with oxaliplatin drug.

Cell culture

HT-1080 human fibrosarcoma cells, were grown at 37°C and 5% CO₂ in Dulbecco's Modified Eagle's Medium (DMEM) supplemented with 10% (v/v) heat-inactivated fetal bovine serum (FBS), 2 mM L-glutamine, 100 U/mL penicillin, and 100 U/mL streptomycin. FBS from obtained from HyClone whereas media and other reagents were from Lonza. Experiments were conducted once cells reached 80-90% confluence.

Flow cytometry analysis

HT1080 cultures were analyzed by flow cytometry techniques. Basically, cultured cells were trypsinized for 5 minutes (0.5% trypsin plus 0.2% EDTA), washed with saline buffer (centrifugation at 600 g, 5 minutes, room temperature) and resuspended in 100 μ L of saline buffer. Cells were incubated with an anti-CD71 monoclonal antibody (M-A712 clone; BD Biosciences). As a negative control, cells were incubated with the same isotype immunoglobulin. After 45 minutes incubation at 4°C in the dark cells were washed and resuspended in 200 μ L of saline buffer.

For cytotoxicity studies, cells were seeded in 24 well plates (BD Biosciences). To test the effect of doxorubicin or oxaliplatin free drugs, medium was replaced with fresh medium containing doxorubicin (Sigma-Aldrich) and cells were further incubated for 48

hours and subjected to flow cytometry analysis. For nanoparticle uptake, cells received fresh medium containing nanoparticle suspensions (0-10 μ g/mL) and were incubated for 24 hours. To release the drugs out of the nanoparticles, cells were first washed with PBS buffer to remove nonspecific binding particles and fresh medium was added to the wells. Photo-responsive experiments were carried out using a BLAK-RAY UV bench lamp (UVP, CA, USA) and the cells were exposed to UV light at 365 nm for 15 min at the distance of ~ 5 cm whereas control plates were untreated. At 2 days post-irradiation, cells were harvested with a trypsin-EDTA solution, resuspended in PBS, stained with Annexin V-APC (BD Biosciences) and 7-AAD (Biolegend) and analyzed by flow cytometry. Data were collected using a FACS Calibur cytometer (BD Biosciences) and analyzed using FlowJo software (Treestar, Ashland, OR, USA).

Confocal microscopy studies

Experiments were conducted in 8-well glass slides (Millipore). For nanoparticle uptake, cells were incubated with medium containing nanoparticle suspensions (0-10 μ g/mL) for 24 hours. The glass slide chambers were completely washed with PBS buffer to remove the non-internalized particles. Then, cells were fixed with 4% paraformaldehyde for 15 min, washed with PBS buffer and stained with Texas Red Phalloidin (Invitrogen). After staining, the slides were rinsed in PBS buffer and mounted in Prolong Gold with DAPI (Invitrogen). The images were acquired using a Leica TCS SP5 confocal microscope (Leica Microsystems, Wetzlar, Germany) equipped with a 63 \times (numerical aperture 1.4) oil immersion objective. Each image cube was optically cut into 16 sections, and the sections that cut through the nucleus and cytoplasm were presented. For presentation purposes, pictures were exported in TIFF format and processed with Adobe Photoshop (Mountain View, CA, USA), for adjustments of brightness and contrast.

Conclusions

In conclusion, a novel nanomaterial able to transport cytotoxic species and release them in response to light irradiation has been presented. In this device, a protein shell anchored on the particle surface through a UV-sensitive cross-linker act as targeting agent and cleavable gatekeeper at the same time. The use of proteins as pore blockers guarantee the biocompatibility of the nanodevice avoiding the use of exotic caps which could provoke toxicity issues in further clinical development steps. This nanocarrier can be internalized by tumoral cells thanks to the presence of transferrin on the external surface and once there, it can release enough amounts of cytotoxic species to initiate the apoptotic cascade in diseased cells after light irradiation. The cytotoxic capacity of this system was evaluated in vitro against several tumoral cell lines which overexpress transferrin receptors, showing an excellent performance being able to transform the diseased cells into apoptotic cells using a very low particle dose. The triggerable high cytotoxic capacity and the versatile nature of the streptavidin/biotin bridges which

allow the introduction of other biotinylated targeting agents, convert this material into a very interesting candidate for the treatment of exposed malignancies accessible by light irradiation. Despite the poor penetration of UV light in living tissues, this system could offer a promising alternative for the treatment of accessible tumors such as skin, esophagus or stomach in which light can be easily applicable by direct irradiation or through the use of optic fiber. Further work is ongoing in order to test the efficacy of this device using *in vivo* murine models.

Acknowledgements

This work was supported by the Ministerio de Economía y Competitividad, through project MAT2012-35556, CSO2010-11384-E (Ageing Network of Excellence), Instituto de Salud Carlos III/Fondos FEDER (PI11/00377FIS), RTICC (RD12/0036/0027) and Comunidad de Madrid (CellCAM; P2010/BMD-2420). M.M.C. thanks CEI Campus Moncloa for the PICATA fellowship. We also thank the X-ray Diffraction C.A.I. and the National Electron Microscopy Center, UCM.

Notes and references

^a Centro de Investigación Biomédica en Red de Bioingeniería, Biomateriales y Nanomedicina (CIBER-BBN). Dpto. Química Inorgánica y Bioinorgánica. UCM. Instituto de Investigación Sanitaria Hospital 12 de Octubre i+12. CEI Campus Moncloa, UCM-UPM, Madrid, Spain. Fax: (+34) 913941786

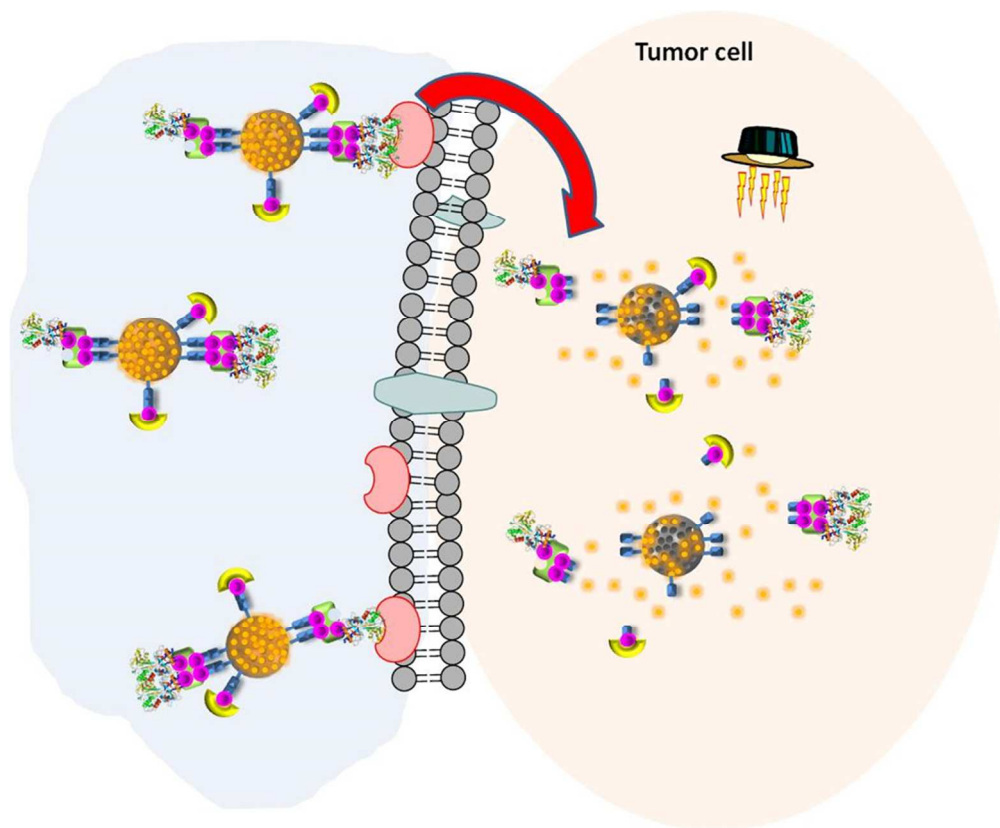
^b Unidad de Biotecnología Celular. Instituto de Salud Carlos III. Crta. Majadahonda-Pozuelo 2. 28220. Madrid, Spain.

* Corresponding authors: abaezaga@ucm.es; vallet@ucm.es

† Electronic Supplementary Information (ESI) available: Experimental proceeds for synthesis of the organic precursors. Additional spectra information; FTIR, NMR, ESI, XRD, BET, size distributions and polydispersity calculations, Flow cytometry analyst of transferrin receptor quantification and cytotoxicity of the oxalilplatin loaded particles. See DOI: 10.1039/b000000x/

- I. Brigger, C. Dubernet, P. Couvreur, *Adv. Drug Deliv. Rev.*, 2012, **64**, 24.
- S.-S. Feng, S. Chien, *Chem. Eng. Sci.*, 2003, **58**, 4087.
- S. D. Steichen, M. Calderera-Moore, N. a Peppas, *Eur. J. Pharm. Sci.*, 2013, **48**, 416.
- R. K. Jain, T. Stylianopoulos, *Nat. Rev. Clin. Oncol.*, 2010, **7**, 653.
- H. Maeda, H. Nakamura, J. Fang, *Adv. Drug Deliv. Rev.*, 2013, **65**, 71.
- J. R. Beech, S. J. Shin, J. A. Smith, K. A. Kelly. *Curr. Pharm. Des.*, 2013, **19**, 6560–6574.
- R. Lehner, X. Wang, M. Wolf, P. Hunziker, *J. Control. Release*, 2012, **161**, 307.
- M. Vallet-Regi, A. Rámila, R. P. del Real, J. Pérez-Pariente, *Chem. Mater.*, 2001, **13**, 308.
- M. Vallet-Regi, F. Balas, D. Arcos, *Angew. Chemie-International Ed.*, 2007, **46**, 7548.
- V. Mamaeva, C. Sahlgren, M. Linden, *Adv. Drug Deliv. Rev.*, 2013, **65**, 689.
- S. Mura, J. Nicolas, P. Couvreur, *Nat. Mater.*, 2013, **12**, 991.
- C. Xu, Y. Lin, J. Wang, L. Wu, W. Wei, J. Ren, X. Qu, *Adv. Healthc. Mater.*, 2013, **2**, 1591.
- E. Ruiz-Hernández, A. Baeza, M. Vallet-Regí, *ACS Nano*, 2011, **5**, 1259.
- A. Schlossbauer, J. Kecht, T. Bein, *Angew. Chem. Int. Ed.*, 2009, **48**, 3092.
- A. Baeza, E. Guisasaola, E. Ruiz-Hernandez, M. Vallet-Regi, *Chem. Mater.*, 2012, **24**, 517.
- E. Aznar, C. Coll, M. Dolores Marcos, R. Martinez-Manez, M. Sancenon, J. Soto, P. Amoros, J. Cano, E. Ruiz, *Chem. Eur. J.*, 2009, **15**, 6877.
- N. Mas, D. Arcos, L. Polo, E. Aznar, S. Sánchez-Salcedo, F. Sancenón, A. García, M. D. Marcos, A. Baeza, M. Vallet-Regí, et al, *Small*, 2014, **10**, 4859.
- S. B. Brown, E. A. Brown, I. Walker, *Lancet. Oncol.*, 2004, **5**, 497.
- A. M. Pekkanen, M. R. Dewitt, M. N. Rylander, *J. Biomed. Nanotechnol.*, 2014, **10**, 1677.
- N. K. Mal, M. Fujiwara, Y. Tanaka, *Nature*, 2003, **421**, 350.
- J. L. Vivero-Escoto, I. I. Slowing, C.-W. Wu, V. S. Y. Lin, *J. Am. Chem. Soc.*, 2009, **131**, 3462.
- N. Z. Knezevic, B. G. Trewyn, V. S. Y. Lin, *Chem. Commun.*, 2011, **47**, 2817.
- N. Ž. Knežević, V. S.-Y. Lin, *Nanoscale*, 2013, **5**, 1544.
- R. Duncan, L. Izzo, *Adv. Drug Deliv. Rev.*, 2005, **57**, 2215.
- D. M. Brown, H. Johnston, E. Gubbins, V. Stone, *J. Biomed. Nanotechnol.*, 2014, **10**, 3416.
- T. Mironava, M. Hadjiargyrou, M. Simon, M. H. Rafailovich, *Nanotoxicology*, 2014, **8**, 189.
- S. Sripriyalakshmi, P. Jose, A. Ravindran, C. H. Anjali, *Cell Biochem. Biophys.*, 2014, **70**, 17.
- K. Peng, I. Tomatsu, B. van den Broek, C. Cui, A. V. Korobko, J. van Noort, A. H. Meijer, H. P. Spaink, A. Kros, *Soft Matter*, 2011, **7**, 4881.
- A. Holmberg, A. Blomstergren, O. Nord, M. Lukacs, J. Lundeborg, M. Uhlen, *Electrophoresis*, 2005, **26**, 501.
- A. Arakaki, S. Hideshima, T. Nakagawa, D. Niwa, T. Tanaka, T. Matsunaga, T. Osaka, *Biotechnol. Bioeng.*, 2004, **88**, 543.
- C. Ocaña, M. del Valle, *Biosens. Bioelectron.*, 2014, **54**, 408.
- T. R. Daniels, E. Bernabeu, J. A. Rodriguez, S. Patel, M. Kozman, D. A. Chiappetta, E. Holler, J. Y. Ljubimova, G. Helguera, M. L. Penichet, *Biochim. Biophys. Acta-General Subj.*, 2012, **1820**, 291.

- 33 Z. M. Qian, H. Li, H. Sun, K. Ho, *Pharmacol. Rev.*, 2002, **54**, 561.
- 34 J. Yue, S. Liu, R. Wang, X. Hu, Z. Xie, Y. Huang, X. Jing, *Mol. Pharm.*, 2012, **9**, 1919.
- 35 C. Sarisozen, A. H. Abouzeid, V. P. Torchilin. *Eur. J. Pharm. Biopharm.*, 2014, **88**, 539–550
- 36 J. Wang, S. Tian, R. A. Petros, M. E. Napier, J. M. DeSimone. *J. Am. Chem. Soc.*, 2010, **132**, 11306–11313.
- 37 D. P. Ferris, J. Lu, C. Gothard, R. Yanes, C. R. Thomas, J.-C. Olsen, J. F. Stoddart, F. Tamanoi, J. I. Zink. *Small*, 2011, **7**, 1816–1826.
- 38 Z. Shao, J. Shao, B. Tan, S. Guan, Z. Liu, Z. Zhao, F. He, J. Zhao. *Int. J. Nanomedicine*, 2015, **10**, 1223–33.
- 39 W. Stöber, A. Fink, E. Bohn, *J. Colloid Interface Sci.*, 1968, **26**, 62.
- 40 A. Baeza, E. Guisasola, A. Torres-Pardo, J. M. González-Calbet, G. J. Melen, M. Ramirez, M. Vallet-Regí, *Adv. Func. Matter.*, 2014, **24**, 4625–4633.
- 41 M. L. Slovak, G. A. Hoeltge, J. M. Trent. *Cancer Res.*, 1987, **47**, 6646–6652.
- 42 A. Salvati, A. S. Pitek, M. P. Monopoli, K. Prapainop, F. B. Bombelli, D. R. Hristov, P. M. Kelly, C. Åberg, E. Mahon, K. a Dawson. *Nanotechnol.*, 2013, **8**, 137–43.
- 43 P. Ponka, C. N. Lok. *Int. J. Biochem. Cell Biol.*, 1999, **31**, 1111–37.



219x180mm (125 x 125 DPI)